A robotic approach based on microgripping for automated experimental tensile testing of natural microfibres

Anouk Chevallier[1*], Ali Zarei[2], Alan Prócel[1], Markus Kakkonen[3], Olli Tanhuanpää[3], Lassi Sukki[2], Florian Boutenel[1], Violaine Guicheret[1], Vincent Placet[1], Pasi Kallio[2*], Cédric Clévy[1*]

[1*]Université Marie et Louis Pasteur, SUPMICROTECH, CNRS, Institut FEMTO-ST, F-25000, Besançon, France.
[2]Faculty of Medicine and Health Technology, Tampere University, Tampere, 33720,Finland.
[3]Fibrobotics Oy, Korkeakoulunkatu 1, 33720, Tampere, Finland.

*Corresponding author(s). E-mail(s): anouk.chevallier@femto-st.fr; pasi.kallio@tuni.fi; cedric.clevy@femto-st.fr;

Abstract

This paper deals with first investigations of a novel approach for conducting tensile tests on single plant fibres using direct microrobotic gripping. These fibres, typically around 20 micrometers in diameter, are gaining significant interest as renewable bio-sourced products. Usual methods for tensile testing generally involve mechanical clamping jaws or adhesive sample holders. This new approach intends to bring greater precision and repeatability of the test through the use of microgrippers, force sensors positioned in close proximity to the fibre and positioning control. A microrobotic experimental platform has been developed. Two different grippers are designed to address the important issue of clamping, the test boundary conditions. Experimental investigations are conducted on 20 tensile tests, validating the viability of the approach. Young's modulus and stress at failure are identified and are in good correspondence with results available in the recent literature of flax fibres. The gripping force exerted by the gripper is a primary factor influencing the repeatability of the test. Therefore, a method is investigated to estimate this force. First experimental results enable to establish that these forces are in tens milliNewton-range forces. This establishes the interest for future works in the design of instrumented grippers able to control gripping forces during tensile tests in closed loop. Overall, this paper states the

interest of a microrobotic approach for tensile tests fibres that opens to several future works including the automation, allowing a large number of fibres to be tested, especially fibres of short length, in order to reduce statistical biases.

Keywords: Gripping, Force measurement, Tensile test, Biobased fibres

1 Introduction

Bio-based composites reinforced with annual plant fibres such as flax offer a reduced environmental footprint compared to composites incorporating synthetic fibres, such as carbon or glass fibres [1–3]. Faced with the need to predict the mechanical performance of these bio-based composites, it is essential to characterise the fibres composing them, particularly in terms of tensile properties. Compared to synthetic fibres, single plant fibres have several specificities of key importance including a intricate morphology and a heterogeneous multilayer microstructure. Their mechanical properties, highly anisotropic, are also linked to their biochemical composition [1, 4]. Thus, the interest in carrying out mechanical characterisation tests at the single fibre level has recently increased. Nevertheless, single flax fibres are also very small (typically diameter in the order of 20 µm) making such tests particularly challenging [5, 6].

Longitudinal Young's modulus, E_L, stress at failure, σ_f, and strain at failure, ε_f, are three crucial parameters required in the design of bio-based composite parts for structural applications. Tensile tests aim to identify them.

A tensile test on a single plant fibre consists of positioning a fibre between two jaws. A tensile force of the order of a hundred milliNewtons is then applied, along with a displacement of no more than a few tens of micrometres. Throughout the test, both tensile force and displacement are measured.

Several works have already investigated experimental measurements based on single plant fibre tensile tests. The reported methods used are mainly of two types. A first one is based on mechanical principles at a reduced scale of jaws where the fibre is clamped. This principle enables a direct clamping of the fibre but, at this scale, alignments appear complex as well as the control of the clamping (boundary conditions of the test) [7]. The second one is based on the use of adhesive with a paper frame, a sample holder [8] or glue droplets [9] that facilitates the clamping of the fibre and alignments. But, this leads to additional sources of uncertainty, particularly concerning the adhesion between glue and fibres or the introduction of glue into the fibres thus modifying the tested object. Both principles, despite their advantages and drawbacks, make it possible to identify Young's modulus, stress and strain at failure, but they require a complex procedure to prepare the fibre in order to successfully carry out the test. Due to the small size of the fibres, the manual handling required during this preparation stage is both time-consuming and delicate, as it poses a risk of misalignment and potential fibre damage.

Moreover, the selected fibres are typically at least one centimetre long, inducing potential statistical biases as only the most mechanically robust and longest fibres are tested [8, 10]. Therefore, it is substantial to enable tests on fibres having a length of few

millimetres [11, 12]. Flax fibres show a higher variability in morphology and mechanical properties compared to their synthetic counterparts [13]. To obtain a statistical representation of this variability, it is essential to carry out a significant number of tests, ideally several hundreds [14]. Consequently, automating the whole process, i.e. more specifically the fibre preparation before testing, the test itself and the post-processing is essential.

To address this key issue, a game changing approach is proposed in this paper, based on microrobotics because it has already demonstrated very promising potential in terms of positioning control [15–17] in natural fibre testing using microgrippers [18–20]. The proposed approach is based on microrobotics and microgrippers used as clamping jaws. This approach offers numerous advantages including a high potential to automate the whole process, the capability to consider all fibres regardless of their morphology and size, preventing from complex handmade test preparation, setting alignments and angles by robot motions in order to reduce the aforementioned statistical biases. In addition, microgrippers enable a direct gripping of the fibres which also simplifies the data processing to identify the mechanical parameters. Grippers have already been used to study the bond strength of pulp fibres [21] but the force magnitude was not as high as in a tensile test.

The aim of this article is therefore to study the potential of the microrobotic approach in tensile testing of single flax fibres to determine the tensile force and displacement involved with control of the jaws geometry. Additionally, the paper introduces a method for measuring the gripping force in the microgrippers used as jaws. For that, an experimental set-up has been developed and is introduced in Section 2.1. First tests have shown that boundary conditions of the fibres during such tests are difficult to control when using gripper fingers with a flat surface in contact with the fibre. This results in slippage for all the tests. To address this important issue, Section 2.1 introduces the design of two specific finger grippers (named Crocodile Gripper (CG) and Wave Gripper (WG)). Section 2.2 then presents the conditions for testing and obtaining the mechanical properties. Section 3 showcases experimental results carried out using these two kinds of grippers and the related Young's modulus and stress at failure identified for flax fibres. Additional experiments to study the possibility of estimating the force with which the fibre is gripped by the gripper are shown in Section 4 . Finally, Section 5 gives concluding remarks and discussions of the work.

2 Materials and methods

2.1 Microrobotic tensile test machine and different grippers

Figure 1 a & b shows the principle of the microrobotic tensile test machine that has been developed at Tampere University. The right jaw is the tested gripper that holds one end of the tested fibre. The type of Actuator B, used to open and close the gripper, varies depending on the gripper being tested (Figure 1 c - e). Linear Actuators D and E and rotary Actuator F allow the fibre to be aligned with the $+\vec{x}$ tensile axis. The other end of the fibre is clamped by compression in the left jaw. The left jaw is screwed to Actuator A which is not operated to open or close the jaw. Force sensor G (Futek LSB200, measuring range: 0 g-100 g) is positioned between the frame and Actuators A

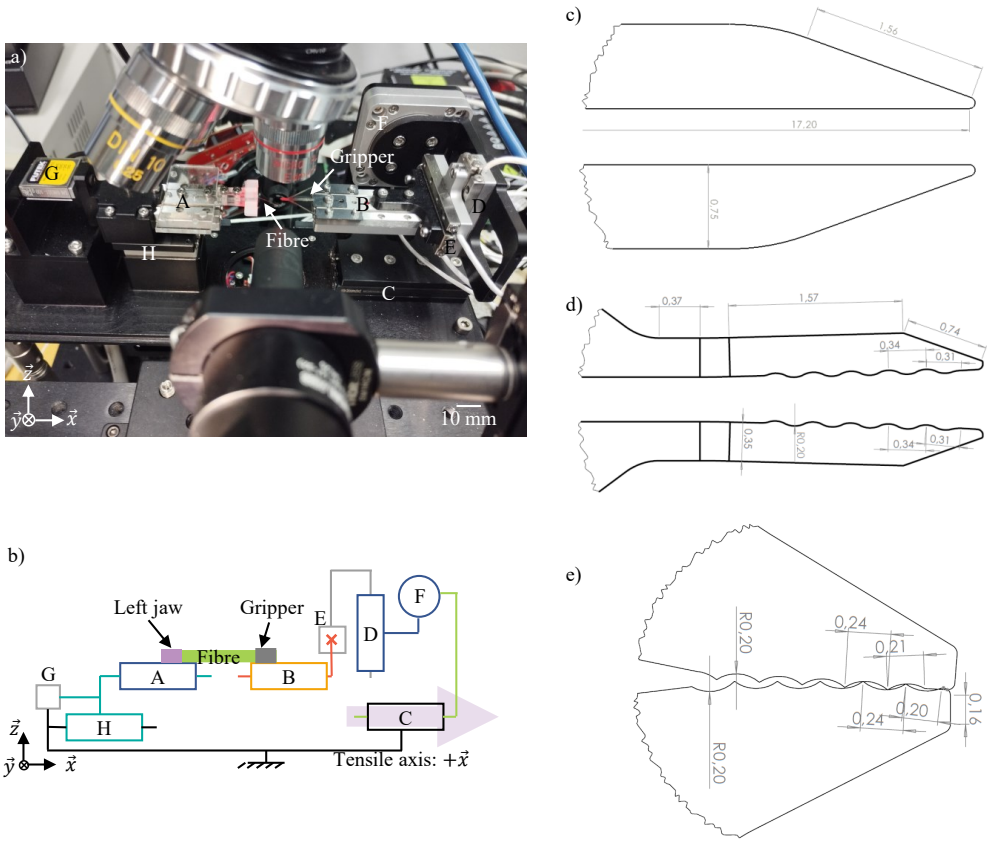

Fig. 1 a) General view of the microrobotic tensile test machine b) Kinematic diagram of the microrobotic tensile test machine with letters referring to the actuators and sensor: A: linear actuator to allow translation along $\vec{x}$ but not moved in this work, B: linear actuator to open and close the gripper, C: linear actuator to allow translation along $\vec{x}$, D: linear actuator to allow translation along $\vec{z}$, E: linear actuator to allow translation along $\vec{y}$, F: rotary actuator to allow rotation around $\vec{y}$, G: sensor to measure force along $\vec{x}$ and H: linear actuator to allow translation along $\vec{x}$ c) Drawing of flat surface finger gripper (unit millimetre) d) Drawing of Wave Gripper (WG-stainless steel) (unit millimetre) e) Drawing of Crocodile Gripper (CG-SU8 polymer) (unit millimetre)

and H. During the tensile test, Actuator A is fixed in relation to Actuator H and the translation of Actuator B in relation to the frame is given by Actuator C. Actuators E, D and F are not actuated during the tensile test.

Two optical microscopes equipped with cameras are used to observe the fibre and the gripper during the test, one along the $\vec{z}$ axis, called top view, and the other along the $\vec{y}$ axis, called side view. Image acquisition frequencies are respectively 40 fps for the side view and 24 fps for the top view.

A critical point in achieving successfully a tensile test on plant fibres lies in the way the fibre is gripped during the tensile test. The gripping force as well as the geometry

of the gripper fingers are key influential parameters. In this paper, different shapes of gripper fingers are investigated.

Figure 1 c-e depicts the three types of gripping system compared. The reference gripper is a flat surface finger gripper, commercially available (SmarAct GmbH, Oldenburg, Germany)(Figure 1 c). The first novel type of gripper (Figure 1 d, designed by Tampere University and manufactured by SmarAct GmbH, is called a Wave Gripper (WG) because the parts that hold the fibre are shaped like two sinusoids that interlock when closed. It is made of stainless steel. It is screwed onto a SmarAct stage (SLC-1740), which is Actuator B (Figure 1 c). The central part of Actuator B slides in relation to the lateral parts. When the central part of the stage moves in one direction, the gripper opens, and closes when the stage moves in the opposite direction. The first point of contact between the two parts holding the fibre is at the tip of the gripper when it closes. They then gradually come into contact along their entire working length. When they are in contact, the tip of the gripper reopens slightly. The second novel type of gripper (Figure 1 e is called a Crocodile Gripper (CG) because the two parts that hold the fibre are shaped like triangular teeth that indent the fibre. They are made of 200 µm thick layer of SU-8 3050 transparent photoresistive epoxy (Kayaku Advanced Materials). They are fabricated on a silicon wafer that is coated with an aluminium sacrificial layer, using standard photolithography techniques, and released via etching process [22]. It is designed and manufactured by Tampere University. It is screwed onto a SmarAct stage (SLC-1730) that takes the place of Actuator B (Figure 1 c). The stage opens and closes the gripper by translating one of the parts while the other remains fixed. When the gripper closes, the first point of contact is at the tip of the gripper, and as the gripper deforms, the contact spreads to the other indentation teeth.

For each gripper, before a series of tensile tests, the left jaw and the gripper are brought into contact in order to visually adjust their position in the $(\vec{x}, \vec{z})$ plane using the side view camera and $(\vec{x}, \vec{y})$ plane by naked eye.

2.2 Test conditions and identification of mechanical properties

Fifty single flax fibres from FlaxTape™ (EcoTechnilin SAS, Valliquerville, France) are isolated and both ends of each are glued onto a paper frame. The gauge length of the tested fibre is approximately 10 mm. An optical microscope (Nikon Eclipse LV150) is used to verify that the flax fibre is a single fibre, with a relatively consistent cross-section along its entire length. One end of the fibre is cut from the paper frame along with the two adjacent sides of the frame. The remaining end of the fibre on the paper frame is clamped onto the left jaw between two surfaces, one made of acrylic and the other made of acrylic but covered with PDMS. The left jaw is then screwed onto Actuator A (Figure 1 b) of the tensile test machine. The free end of the fibre is gripped with the gripper, cleaned with a brush, trying to have the same length (approximately 700 µm) of fibre gripped inside the gripper in all cases (flat, WG, CG). For all grippers, the gripping force level is experimentally determined to avoid failure of the fibre in the gripper by trial and error tests; it is then set to the same stage position for all the tensile tests.

Throughout the tests, the temperature is $22.2 \pm 0.7\,^{\circ}\mathrm{C}$ and the relative humidity in the room is $21.6 \pm 3.5\,\%$. The tensile test is performed with a displacement speed of $16\,\mu\mathrm{m\,s^{-1}}$, recording tensile force, displacement of the Actuator C (Figure 1) and both top and side camera images. When the fibre breaks, if it is possible, the free end of the fibre that has just broken is glued onto a piece of paper in order to move for microscope observation. Ten fibres per type of gripper are tested (WG and CG). The remaining fibres were employed for training to the use of the tensile test machine and fine-tuning the experimental protocol. Following the tensile test, the remaining part or parts of the fibre are observed under a digital microscope (Keyence VHX-5000). Assuming the cross-section of the fibres is circular, their diameters are measured in three zones, each distributed approximately evenly along the initial length of the fibre.

- Zone 1 is always joined to the left jaw
- Zone 3 is always in the compressed region in the gripper

In case of failure:

- Zone 2 is positioned in the centre of the left part of the fibre clamped to the left jaw

Notice that the position of Zone 2 depends on the location of the failure point. For some fibres, it may not be feasible to measure in certain zones due to the remaining part being too small to be collected after failure.
In case of slippage, Zone 2 is in the middle of the fibre.

To work out the stress ($\sigma = \frac{F}{A}$ where F is the recorded tensile force and A the area of the cross-section of the fibre), the average of the diameters measured in Zone 1 and Zone 2 is used. If measurement either in Zone 1 or in Zone 2 is unavailable, the diameter measured in another zone is used. The strain ($\epsilon = \frac{\Delta L}{L}$ where ΔL is the change in fibre gauge length and L the initial gauge length of the fibre) is derived from the displacement measured without compliance correction, considering the initial length of the fibre as 10 mm. Young's modulus, the slope of stress σ vs strain ε curve, is determined within the strain range of $0.15\,\%$ to $0.35\,\%$.

3 Results and discussion

Several events can occur during a tensile test. The fibre can break at different points such as in its gauge section or close to the clamps. The gauge section is defined as the section that is not contiguous to the jaw nor to the gripper (Figure 2).

For the tensile tests carried out in this study, the gauge section corresponds to the eight millimetres in the centre of the fibre (one millimetre discarded at each end). According to the standard [23], a test is valid when the fibre breaks in the gauge section. Longitudinal Young's modulus and stress at failure are therefore identified for these fibres. Conversely, when the failure is close to the clamp, the test is not considered valid by the standard. In fact, the measured tensile stress is only one component of the possible multiaxial stresses leading to fibre failure.

During a tensile test, the fibre can also slip in the jaws. The displacement measured in this case is not a displacement that produces a tensile force on the fibre.

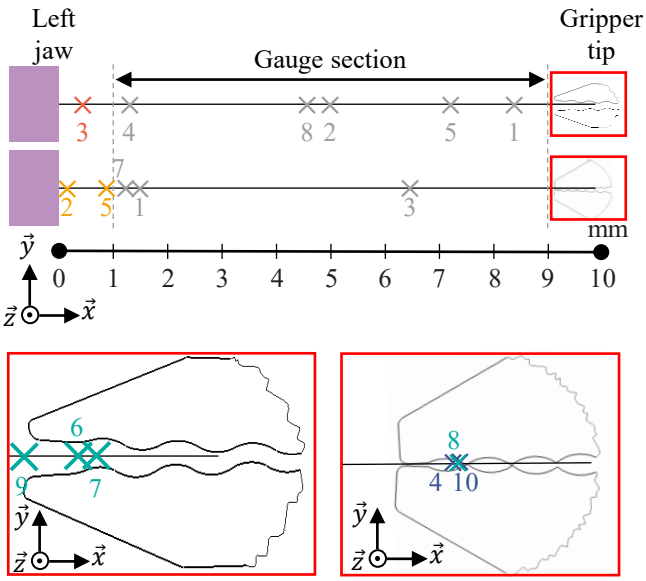

Fig. 2 Approximated failure points and zone in which these points are located

However, only the displacement producing a tensile force on the fibre is included in the calculation of the strain [24]. According to the standard, this test should therefore be discarded.

The number of each scenario, i.e. the characteristic test events observed during ten tensile tests for each gripper (slippage and/or failure of the fibre at a given location), is shown in Figure 3 a. These observations are made possible by the two microscopes installed on the tensile test machine. Primarily, the incidence of slip-free tests is notably higher with these grippers compared to flat fingers, as the latter consistently experienced some level of slippage making it impossible to use them as gripping jaws in a tensile test. Among the ten fibres tested with each gripper, respectively five for the WG and three for the CG broke in the gauge section. The results obtained with the WG therefore appear more promising.

The tensile force/displacement curves are drawn in Figure 3 b and c. Each curve is color-coded, based on the zone where the failure point is observed and the scenario witnessed during the test. For some curves, a sudden decrease (not leading to a zero force) in the measured tensile force is observed. This corresponds to the slippage of the fibre within the gripper which is confirmed by the visual feedback from the two cameras on the microrobotic tensile test machine.

The Young's modulus of each fibre tested is identified from its tensile force/displacement curve and from the diameter measurements taken after testing, i.e. for an elastic behaviour, the longitudinal Young's modulus E is the slope of the stress/strain curve ($\sigma = E\epsilon$). For all tested fibres, the longitudinal Young's modulus can be determined within the range 0.15 % and 0.35 % of strain, as slippage only occurs outside this range. The stress at failure is identified for the scenarios where the fibre fails in

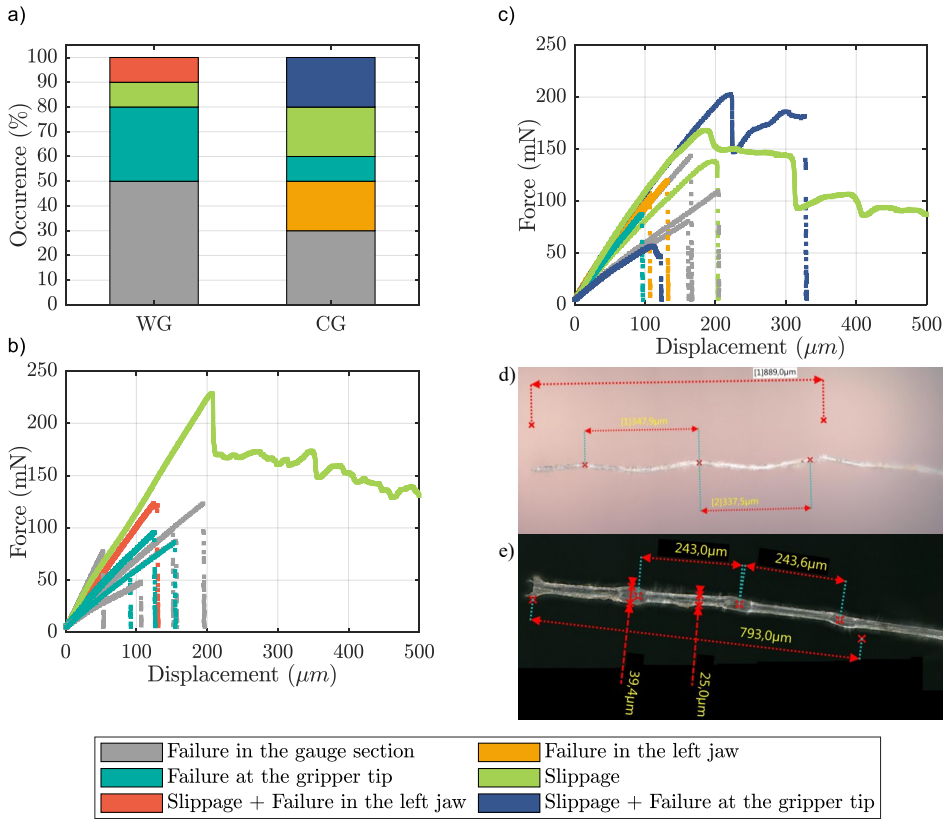

Fig. 3 a) The different scenarios emerging during tensile tests on ten flax fibres per type of gripper, tensile force/displacement curves obtained with b) WG and c) CG & example of a fibre in the gripping zone after the tensile test, tested d) with the WG and e) with the CG

the gauge section. When the fibre slips inside the grippers during the test and does not break, the maximum stress measured is a lower bound of the stress at failure. The same applies if the fibre first slips inside the grippers and then breaks as well as when the fibre breaks in the left jaw or at the gripper tip.

Table 1 shows the values of Young's moduli and stresses at failure identified for the fibres tested with each gripper. For WG, the mean Young's modulus and stress at failure are 40.2 ± 20.2 GPa and 622 ± 422 MPa, respectively. For CG, the mean Young's modulus and stress at failure are 43.2 ± 18.5 GPa and 942 ± 198 MPa, respectively. These values are in line with the literature: the flax fibre Young's modulus is in the range of 46.9 ± 15.7 GPa to 68.2 ± 35.8 GPa and its stress at failure is in the range of 850 ± 359 MPa [13]. However, care must be taken with the cross-sectional measurement of the fibre retained [25], notably three fibres with a higher Young's modulus and/or

stress at failure are, for this reason, considered as outliers. This validates the use of grippers with a specific geometry for flax fibre tensile test.

Nonetheless, the fibre often slips in the gripper: for instance two fibres out of ten for the WG and four out of ten for the CG. Only one parameter influencing this scenario could be fully identified experimentally. It is observed on the tensile force/displacement curves (Figure 3 b and c) that with both grippers tested, excessive tensile force leads to slippage. Specifically, slippage occurs at approximately 130 mN for the WG and approximately 168 mN for the CG. To address the issue of slippage, Zarei et al. [26] proposed a machine learning-based method to predict whether a fibre will slip when gripped by two grippers prior to a tensile test. This method uses images of the fibre within the grippers as well as the positions of the stages as input data.

Figure 3 d & e shows microscope images, after a tensile test, of the fibre region clamped into the gripper. For the WG type, the part of the fibre clamped in the gripper is shaped like the same wave as the gripper and appears to be irreversibly deformed (Figure 3 d. In the case of the CG, the damaged areas are at the indentation points, where a shear stress appears. That results in local flattening of the fibre (Figure 3 e. Consequently, these fibre deformations could be the cause of failures at the gripper tip. On CG, after fibre slippage in the grippers, fibre failure can also be observed at the indentation points preceding slippage. The shape of the grippers, especially the WG, has a good potential for tensile testing but could be improved in future works, for example by increasing the coefficient of friction between the fibre and the finger gripper or by controlling the gripping force of the fibre in the grippers.

4 Gripping force estimation

In addition to the tests conducted at Tampere University (Finland), complementary experiments were performed at FEMTO-ST Institute (France) to explore the possibility of estimating gripping force from displacement data. Such information would help avoid excessive force that could damage the fibre or insufficient force that might lead to fibre slippage. This would lead to improve the single fibre tensile test repeatability. Direct measurement of the gripping force during the tensile test is challenging because commercial force sensors are too bulky to measure forces directly between the two gripper fingers. For this purpose, a force estimation method is developed, based on two phases of analysis and experimentation. In the first phase, an analytical model is developed in order to estimate the force applied by a gripper finger when the gripper opens. This model is experimentally validated with a reference force sensor that is temporarily used for this phase. In the second phase, the model is used to estimate the gripping force on a flax fibre when compressed by the gripper.

4.1 Analytical model of the force applied by a gripper finger

The aim of this section is to analyse the gripper finger tip's displacement as the resulting effect of the applied force and the input displacement of the stage that allows the gripper opening and closing. To achieve this, an experimental setup is designed to simultaneously measure the finger gripper tip position, $Y1$, and the applied force,

Table 1 The identified Young's modulus (E_L) and stress at failure (σ_f)

Fibre no.	Scenario	E_L GPa	σ_f MPa
	WG		
1	Failure in the gauge section	66.0	1 013
2	Failure in the gauge section	26.3	403
3	Slippage + Failure in the left jaw	58.5	$\geq$ 704
4*	Failure in the gauge section	203.4	1 119
5	Failure in the gauge section	24.7	431
6 **	Failure at the gripper tip		
7*	Slippage	141.0	$\geq$ 2 527
8	Failure at the gripper tip	35.1	423
9	Failure in the gauge section	13.8	144
10	Failure at the gripper tip	57.0	828
		40.2 $\pm$ 20.2	622 $\pm$ 422 ***
	CG		
1	Failure in the gauge section	67.3	1 007
2 *	Failure in the left jaw	116.5	1 220
3	Failure in the gauge section	72.9	1 100
4	Slippage + Failure at the gripper tip	27.4	$\geq$ 500
5	Failure in the left jaw	42.6	500
6	Slippage	39.2	$\geq$ 640
7	Failure in the gauge section	37.5	720
8	Failure at the gripper tip	54.6	510
9	Slippage	30.4	440
10	Slippage + Failure at the gripper tip	17.2	$\geq$ 180
		43.2 $\pm$ 18.5	942 $\pm$ 198 ***

*Outliers not considered.

**Impossible to measure the diameter.

***Only considering failure in the gauge section.

Fm, while controlling the input position of the stage Xa, that allows the opening and closing of the gripper.

Supplementary information 1 (Figure 1) shows this experimental setup. It involves a gripper screwed onto a SmarAct stage (SG17030S-19) controlling the input position Xa, a force sensor (TEI FSB101, measuring range: ± 0.1 N) positioned perpendicular to the gripper, and a reflection laser sensor (KEYENCE LC-2420, resolution: 0.01 µm) to measure the position of the gripper finger tip, $Y1$. An intermediate plate is glued, on the finger gripper tip, at the contact point between the force sensor and the gripper, to measure its displacement directly with the laser. The SmarAct stage moves in 0.3 µm steps. The stage position is held for 5 s. The Xa and $Y1$ positions are sampled at 20 Hz and 40 Hz, respectively. For each step, the mean value of Xa and $Y1$ are plotted.

Figure 4 shows the evolution of the position of the gripper finger tip, $Y1$, as a function of the input position, Xa, when opening the gripper. In this figure, the following can be identified:

- $m1$ is the slope of the line before the contact between the gripper finger tip and the force sensor (free motion of the finger, $Fm = 0$).
- $m2$ is the slope of the line after the contact between the gripper finger tip and the force sensor (constrained motion, $Fm \neq 0$ and $Y1 \neq 0$).

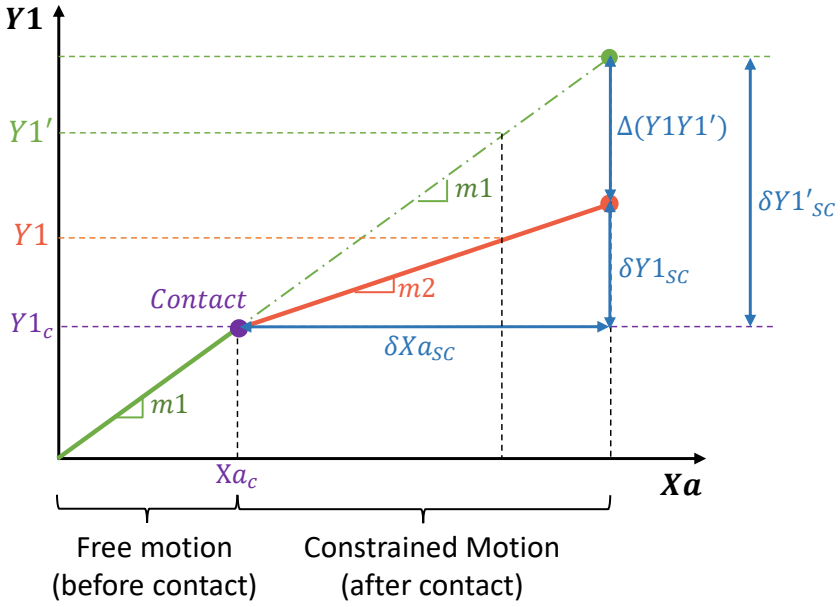

Fig. 4 Example of the curve obtained from experimental measurement of $Y1$ (gripper finger tip position) vs Xa (input position)

- $Y1'$ is the position of the finger gripper tip if there were no contact between the force sensor and the gripper finger tip i.e. the gripper finger tip were in free motion
- The contact point between the gripper finger and the force sensor is at $(Xa_c, Y1_c)$.

Figure 5 presents the equivalent schematic of the force sensor and the finger gripper before contact, at contact and after contact between them. The reference force sensor is assumed to be modelled as a spring with an apparent stiffness denoted k_{sensor}. The gripper finger, a compliant structure made of silicon, is also assumed to be modelled as a spring, with an apparent stiffness at the contact point with the force sensor denoted k_{gp_1}. After contact, when the gripper opens the spring is compressed while when the gripper closes, it is extended. After contact, these two springs modelling the force sensor and the gripper finger are in series. Until the contact between the force sensor and the gripper finger, the applied force, F_m, is zero and the position of the finger gripper tip, $Y1$, follows the $m1$ slope line in Figure 4, so $Y1 = m1 \times Xa$. After the contact, the position of the gripper finger tip, $Y1$, follows the $m2$ slope line in Figure 4, so $Y1 = m2 \times Xa$. As shown in Figures 4 and 5, from the contact point, the tip of the gripper finger moves a distance called $\delta Y1_{SC}$ (displacement of the point $Y1$ since contact) i.e. $\delta Y1_{SC} = Y1 - Y1_c$. If the movement of the gripper finger were free, this distance would be $\delta Y1'_{SC} = Y1' - Y1_c$. Therefore, there is a difference between the expected position $Y1'$ and the actual measured position $Y1$, denoted $\Delta(Y1Y1')$, i.e. $\Delta(Y1Y1') = Y1' - Y1$. Considering the assumption of the gripper and force sensor as two springs in series after contact, shown in Figure 5, and the distances identified

in Figure 4, the relations (1), (2), (3) and (4) can be established. Table 2 summarizes all the variables involved in the analytical model.

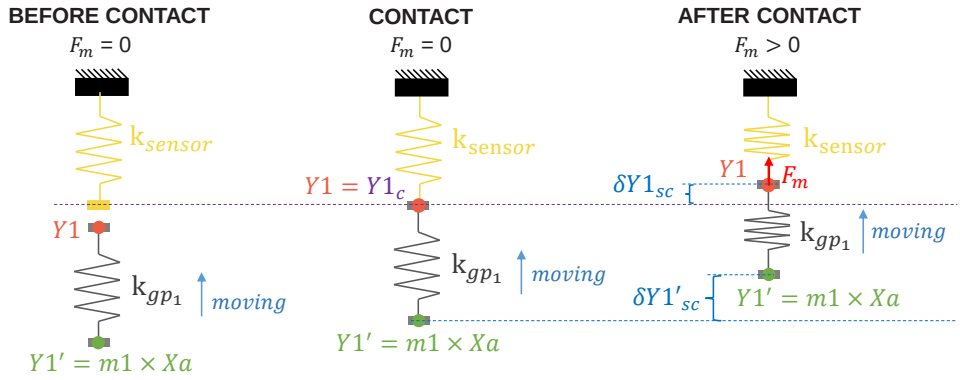

Fig. 5 Equivalent schematic before contact, at contact and after contact between gripper and force sensor

Table 2 Summary of variables involved in gripping force

Variable	Description
Xa	Input position, position measured by the internal sensor of the SmarAct stage
$Y1$	Position of the gripper finger tip, measured by the laser
$Y1'$	Expected position of the gripper finger if contact never happens
$\Delta(Y1Y1')$	Distance between $Y1$ and $Y1'$
$\delta Y1_{SC}$	Displacement of point $Y1$ since contact
$\delta Y1'_{SC}$	Displacement of point $Y1'$ since contact
F_m	Applied force at $Y1$, measured by the force sensor
k_{sensor}	Apparent force sensor stiffness
k_{gp_1}	Apparent gripper finger stiffness
k_{eq}	Equivalent stiffness of force sensor and the gripper finger
$m1$	Slope in $Y1$ vs Xa curve before the contact
$m2$	Slope in $Y1$ vs Xa curve after the contact

$$\delta Y1_{SC} = \frac{F_m}{k_{sensor}} \tag{1}$$

$$\Delta(Y1Y1') = \frac{F_m}{k_{gp_1}} \Leftrightarrow F_m = k_{gp_1} \times (m1 \times Xa - Y1) \tag{2}$$

$$\delta Y1'_{SC} = \frac{F_m}{k_{eq}} \tag{3}$$

where,

$$k_{eq} = \frac{k_{sensor} \times k_{gp_1}}{k_{sensor} + k_{gp_1}} \tag{4}$$

The input displacement, Xa, the force Fm and the position of finger gripper tip, $Y1$ are experimentally measured. This allows to deduce $Y1_c$, $\delta Y1_{SC}$, $\delta Y1'_{SC}$ and $\Delta(Y1Y1')$. From relation (1) the apparent stiffness of the force sensor, k_{sensor}, is identified. Relation (2) allows the identification of the gripper finger apparent stiffness, k_{gp_1}. As relations (3) and (4) are satisfied by the obtained apparent stiffnesses, and the experimental curve in Supplementary information 2 Figure 2 is consistent with the model developed and represented in Figure 4, the assumption that the finger gripper and the force sensor can be modelled as two springs in series is valid. The apparent stiffness of the gripper finger, k_{gp_1} is $14.83 \pm 1.44\,\mathrm{kN\,m^{-1}}$.

4.2 Application of the model for single fibre gripping force estimation

In the second phase, the aim is to estimate the gripping force (F_g) over a flax fibre, using the model previously developed. As the gripper finger, whether the gripper is opening or closing, is modelled by a spring of apparent stiffness k_{gp_1}, the force Fm considered in Section 4.1 can be replaced by the force F_g. Figure 6-a shows the experimental setup used, where the force sensor has been removed, and a single flax fibre is inserted into the gripper.

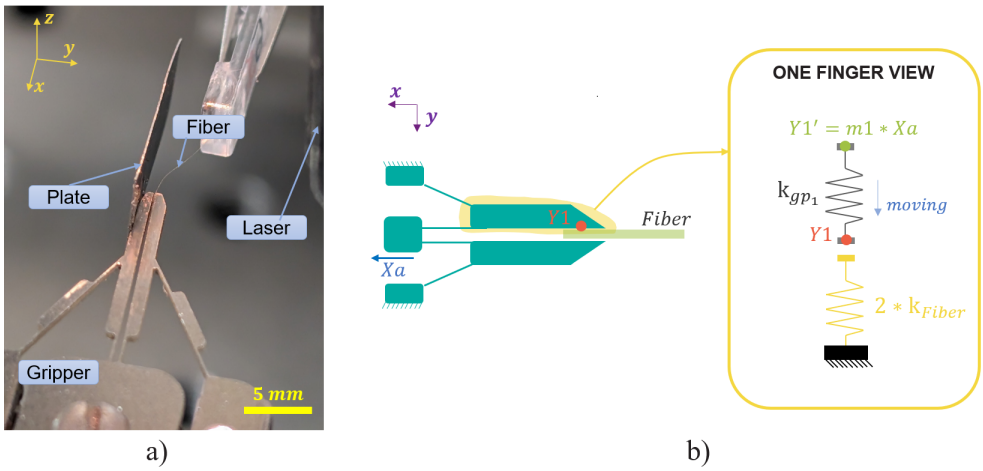

Fig. 6 Experimental setup for the estimation of gripping force on a plant fibre: (a) Picture of the elements involved (b) Equivalent schematic of the system

Relationship (2) is used to estimate the gripping force F_g without using the apparent stiffness of the fibre, k_{fiber}, as shown in relationship (5).

$$F_g = k_{gp_1} \times \Delta(Y1Y1') = k_{gp_1} \times (Y_1' - Y_1) \tag{5}$$

where,

$$Y_1' = m1 \times X_a \tag{6}$$

It is now possible to calculate F_g from the experimental position measurements. Figure 7-a shows the experimentally measured evolution of the input position, Xa, as a function of the finger gripper tip position, $Y1$. In figure 7-b, this curve is used to determine, using linear fits, the slope, $m1$, of the line before contact, and the slope, $m2$, of the line after contact. Finally, Figure 7-c shows the evolution of the estimated gripping force F_g as a function of the input displacement Xa.

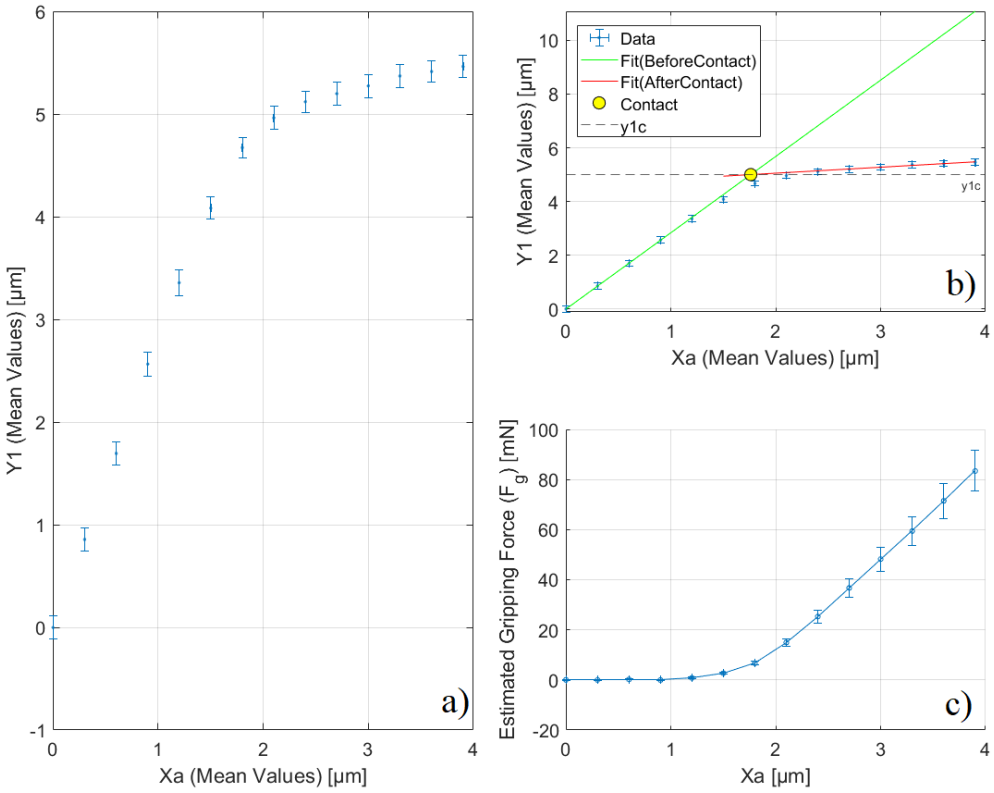

Fig. 7 (a) Measurements obtained from fiber gripping experiment (b) Curve analysis and $m1$ estimation for later obtaining $\Delta(Y1Y1')$ (c) Resulting gripping force estimation for the experiment

Therefore, the gripping force can be estimated using the displacement data of the stage that closes the gripper.

A final experiment combining simultaneously measurement of the tensile force and an estimator of the gripping force is performed. In two tensile tests carried out with a flat surface finger gripper applying gripping forces of around 50 mN and 100 mN, slippage occurs at a tensile force of 2.5 mN and 21.7 mN respectively. It seems that

the greater the gripping force, the greater the tensile force leading to fibre slippage. Our measurements indicate that the maximum gripping force achievable by these flat surface fingers is approximately 100 mN, beyond which the finger tips begin to reopen. The curve showing the evolution of the estimated gripping force as a function of the input position can be found in Supplementary information 3 Figure 3.
Regarding the specifications of the manufacturers of the SmarAct stage for Xa and the Keyance reflection laser sensor for $Y1$, the uncertainty on the estimated gripping force Fg is evaluated around 10% using the norm proposed by the Bureau International des Poids et Mesures [27]. The performed experiment highlights that the gripping forces are in the order of hundreds of milliNewtons. Additionally, the relative stiffness of the fibre to the stiffness of the gripper structure is well-conditioned to enable in real-time, gripping force estimation and potentially even the force control within a few milliNewtons. This level of precision in both estimated gripping force and input displacement Xa, offers a promising tool for improving the accuracy of microrobotic tensile testing, with also great potential for application in mechanical characterisation of fibres.

Moreover, this model can be used to measure the fibre stiffness. By analogy with the first phase, in Figure 5, the spring modelling the apparent stiffness of the force sensor, k_{sensor}, is replaced by a spring modelling twice the stiffness of the fibre, k_{fibre}. As a single finger has a $\delta Y1_{SC}$ displacement, $2\delta Y1_{SC}$ is displacement for the two gripper fingers displacement during gripping i.e. $\delta fb_c = 2 \times \delta Y1_{SC}$. Therefore relation (1) becomes relation (7).

$$\delta Y1_{SC} = \frac{\delta fb_c}{2} = \frac{F_g}{2 \times k_{fibre}} \Leftrightarrow k_{fibre} = \frac{F_g}{2 \times \delta Y1_{SC}} \tag{7}$$

5 Conclusion

The aim of this article is to investigate the potential benefits of using a microrobotic approach to carry out tensile tests on plant fibres, which are particularly small (diameter in the order of 20 µm). To this purpose, an experimental microrobotic platform has been developed at Tampere University (Finland). It is equipped with microgrippers for clamping the fibre and then carrying out tensile tests. As a fibre always slips from a flat finger gripper, two specific forms of gripper have been studied to ensure good control of fibre embedding conditions during the tests. Series of ten tensile tests for each type of gripper was successfully carried out. All these tests prove to be workable, enabling us to identify the longitudinal Young's modulus and the stress at failure. The values obtained are in line with the data available in the literature, enabling to validate the potential of this microrobotic approach. This approach also seems relevant for the mechanical characterisation of synthetic fibres such as carbon, glass as well as hair for the cosmetics industry.

Complementary experiments are also performed in FEMTO-ST Institute (France) to estimate the gripping force using displacement data of the stage that allows the opening and closing of the gripper. A relationship between the applied force and the apparent stiffness of the gripper is established and experimentally verified using force measurements. This relationship is successfully applied to estimate the gripping force

on a flax. This offers a promising tool for improving the accuracy and repeatability of microrobotic tensile tests.

These results propose an innovative alternative to the currently available methods, as they enable to envision significant facilitation of the entire process, from fibre preparation to testing and data analysis. Also, these tests can be largely automated, making it possible to carry out much larger and statistically richer test campaigns. This new approach to robotic automation will also resolve known statistical biases for which no solution is found yet.

Acknowledgements. This work is supported by the Région Bourgogne Franche-Comté, the FEMTO-ST scientific board for the student ambassador award as well as the Université de Franche-Comté for the "Mobilité Internationale des Doctorants" grant. This work has been partially funded by the DYNABOT Project (ANR-21-CE10-0016), the EIPHI Graduate School (ANR-17-EURE-0002) and the French RENATECH and ROBOTEX networks (TIRREX ANR-21-ESRE-0015) through their FEMTO-ST technological facilities MIMENTO, MIFHySTO and CMNR.
The research leading to these developments has received funding from the European Union's Horizon 2020 research and innovation programme under the Marie Skłodowska-Curie grant agreement No 764713 (FibreNet), and from the doctoral education programme of Faculty of Medicine and Health Technology at Tampere University. We also acknowledge Fibrobotics Co. for designing the hardware platform.

References

[1] Bourmaud, A., Beaugrand, J., Shah, D.U., Placet, V., Baley, C.: Towards the design of high-performance plant fibre composites. Progress in Materials Science **97**, 347–408 (2018) https://doi.org/10.1016/j.pmatsci.2018.05.005

[2] Pickering, K.L., Efendy, M.A., Le, T.M.: A review of recent developments in natural fibre composites and their mechanical performance. Composites Part A: Applied Science and Manufacturing **83**, 98–112 (2016) https://doi.org/10.1016/j.compositesa.2015.08.038

[3] Ramesh, M.: Flax (linum usitatissimum l.) fibre reinforced polymer composite materials: A review on preparation, properties and prospects. Progress in Materials Science **102**, 109–166 (2019) https://doi.org/10.1016/j.pmatsci.2018.12.004

[4] Chokshi, S., Parmar, V., Gohil, P., Chaudhary, V.: Chemical composition and mechanical properties of natural fibers. Journal of Natural Fibers **19**(10), 3942–3953 (2022) https://doi.org/10.1080/15440478.2020.1848738

[5] André, A.N., Lehmann, O., Govilas, J., Laurent, G.J., Saadana, H., Sandoz, P., Gauthier, V., Lefevre, A., Bolopion, A., Agnus, J.: Automating robotic microassembly of fluidic chips and single fiber compression tests based-on xytheta visual

measurement with high-precision fiducial markers. IEEE Trans. on Automation Science and Engineering (2022) https://doi.org/10.1109/TASE.2022.3218686

[6] Govilas, J., *et al.*: Platen parallelism significance and control in single fiber transverse compression tests. Composites Part A: Applied Science and Manufacturing **159**, 106990 (2022) https://doi.org/10.1016/j.compositesa.2022.106990

[7] Žižek, M., Czibula, C., Hirn, U.: How the test setup can affect single fiber tensile testing. Journal of Natural Fibers **21**(1), 2328264 (2024) https://doi.org/10.1080/15440478.2024.2328264

[8] Mesquita, F., Bucknell, S., Leray, Y., Lomov, S.V., Swolfs, Y.: Single carbon and glass fibre properties characterised using large data sets obtained through automated single fibre tensile testing. Composites Part A: Applied Science and Manufacturing **145**, 106389 (2021) https://doi.org/10.1016/j.compositesa.2021.106389

[9] Ren, D., Yu, Z., Li, W., Wang, H., Yu, Y.: The effect of ages on the tensile mechanical properties of elementary fibers extracted from two sympodial bamboo species. Industrial Crops and Products **62**, 94–99 (2014) https://doi.org/10.1016/j.indcrop.2014.08.014

[10] Amroune, S., Belaadi, A., Bourchak, M., Makhlouf, A., Satha, H.: Statistical and experimental analysis of the mechanical properties of flax fibers. J. of Natural Fibers **19**(4), 1387–1401 (2022) https://doi.org/10.1080/15440478.2020.1775751

[11] Ganesh, R., Obaid, A.A., Gillespie Jr, J.W.: Experimental determination of bimodal strength distribution of s-glass fibers. Composites Part B: Engineering **254**, 110559 (2023) https://doi.org/10.1016/j.compositesb.2023.110559

[12] Pardini, L.C., Manhani, L.G.B.: Influence of the testing gage length on the strength, young's modulus and weibull modulus of carbon fibres and glass fibres. Materials research **5**, 411–420 (2002) https://doi.org/10.1590/S1516-14392002000400004

[13] Richely, E., *et al.*: A critical review of the ultrastructure, mechanics and modelling of flax fibres and their defects. Progress in Materials Science **124**, 100851 (2022) https://doi.org/10.1016/j.pmatsci.2021.100851

[14] Joannès, S., Islam, F., Laiarinandrasana, L.: Uncertainty in fibre strength characterisation due to uncertainty in measurement and sampling randomness. Applied Composite Materials **27**, 165–184 (2020) https://doi.org/10.1007/s10443-020-09803-9

[15] Yao, S., Zhang, X., Zhu, B., Li, H., Yu, L., Fatikow, S.: A microvision-based motion measurement system for nanopositioners using the feature-to-phase method. IEEE Transactions on Instrumentation and Measurement **72**, 1–11

(2023) https://doi.org/10.1109/TIM.2023.3234038

[16] Adam, G., et al.: An overview of microrobotic systems for microforce sensing. Annual Review of Cont., Rob., and Auton. Syst. **7** (2024) https://doi.org/10.1146/annurev-control-090623-115925

[17] Adam, G., Ulliac, G., Clevy, C., Cappelleri, D.J.: 3d printed vision-based microforce sensors for microrobotic applications. Journal of Micro and Bio Robotics **18**(1), 15–24 (2022) https://doi.org/10.1007/s12213-023-00152-x

[18] Komati, B., Kudryavtsev, A., Clévy, C., Laurent, G., Tamadazte, B., Agnus, J., Lutz, P.: Automated robotic microassembly of flexible optical components. In: Int. Symp. on Ass. and Manuf., pp. 93–98 (2016). https://doi.org/10.1109/ISAM.2016.7750721 . IEEE

[19] Hannouch, R., Reynaud, V., Colas, G., Rauch, J.-Y., Agnus, J., Lehmann, O., Marionnet, F., Clevy, C.: In-situ sem microrobotics for versatile force/deformation characterization: application to third-body m o s 2 wear particles, vol. 20, p. 7. Springer, ??? (2024). https://doi.org/10.1007/s12213-024-00172-1

[20] Tiwari, B., Ghorbani, M., Cisier, D., Perriard, Y.: Towards development of a novel variable stiffness instrumented gripper. In: Int. Conf. on Control, Mechatronics and Automation, pp. 392–396 (2023). https://doi.org/10.1109/ICCMA59762.2023.10374678 . IEEE

[21] Saketi, P., Latifi, S.K., Hirvonen, J., Rajala, S., Vehkaoja, A., Salpavaara, T., Lekkala, J., Kallio, P.: Pvdf microforce sensor for the measurement of z-directional strength in paper fiber bonds. Sensors and Actuators A: Physical **222**, 194–203 (2015) https://doi.org/10.1016/j.sna.2014.12.003

[22] Salpavaara, T., Joki, T., Skogberg, A., Calejo, M., Lekkala, J., Narkilahti, S., Kallio, P.: Microfabricated porous su-8 membranes as innervation interfaces for hipsc-neurons in microfluidic devices. Journal of Physics Communications **5**(11), 115003 (2021) https://doi.org/10.1088/2399-6528/ac314d

[23] Fibres de renfort Fibres de lin pour composites plastiques Partie 2 : Détermination des propriétés en traction des fibres élémentaires. Standard NF T25-501-2, Association Française de Normalisation (AFNOR) (March 2015)

[24] Engelbrecht-Wiggans, A.E., Forster, A.L.: Analysis of strain correction procedures for single fiber tensile testing. Composites Part A: Applied Science and Manufacturing **167**, 107411 (2023) https://doi.org/10.1016/j.compositesa.2022.107411

[25] Aslan, M., Chinga-Carrasco, G., Sørensen, B.F., Madsen, B.: Strength variability of single flax fibres. Journal of materials science **46**, 6344–6354 (2011) https://doi.org/10.1007/s10853-011-5581-x

[26] Zarei, A., Rajan, D.K., Kallio, P.: Slippage prediction in microrobotic fiber characterization. In: 2024 IEEE 20th International Conference on Automation Science and Engineering (CASE), pp. 3975–3982 (2024). https://doi.org/10.1109/CASE59546.2024.10711614 . IEEE

[27] Joint Committee for Guides in Metrology: Evaluation of Measurement Data – Guide to the Expression of Uncertainty in Measurement (GUM 1995 with Minor Corrections). (2008). JCGM 100:2008